CSAWAC 44 (8) 909-1084 (2016) · Vol. 44 · No. 8 · August 2016

CLEAN
Soil Air Water

Renewables

Sustainability

Environmental Monitoring

8 | 2016

www.clean-journal.com

WILEY

CLEAN
Soil Air Water

Yasin Ozay[1]
Nadir Dizge[1]
Habibe Elif Gulsen[1]
Ceyhun Akarsu[1]
Ersan Harputlu[2]
Erman Ozer[3]
Ali Unyayar[1]
Kasim Ocakoglu[2,4]

[1]Department of Environmental Engineering, Mersin University, Yenisehir, Mersin, Turkey
[2]Advanced Technology Research and Application Center, Mersin University, Yenisehir, Mersin, Turkey
[3]Department of Biotechnology, Mersin University, Yenisehir, Mersin, Turkey
[4]Faculty of Technology, Department of Energy Systems Engineering, Mersin University, Mersin, Turkey

Research Article

Investigation of Electroactive and Antibacterial Properties of Polyethersulfone Membranes Blended With Copper Nanoparticles

In this study, copper nanoparticles (CuNPs) were synthesized by sonochemical reduction of copper(II) hydrazine carboxylate complex in an aqueous medium. Asymmetric neat polyethersulfone (PES) and PES/CuNPs nanocomposite membranes were prepared via phase inversion method by dispersing copper nanoparticles in the PES casting solutions. X-ray diffraction and particle size distribution analyses were applied to characterize the CuNPs. Moreover, field emission scanning electron microscopy, atomic force microscopy (AFM), conductive atomic force microscopy (C-AFM), contact angle goniometry, and four-point probe techniques were used to investigate the physical and morphological properties of the PES/CuNPs nanocomposite membranes. Synthesized CuNPs were added into the casting solution at different concentrations. The effect of CuNPs concentration (0, 0.25, 0.5, 1.0, 2.0%, w/w) was tested on morphological changes and antibacterial properties of the prepared membranes. These copper nanoparticle composite membranes hold great promise in the engineering field for the production of sensors and self-cleaning membranes.

Keywords: Antibacterial performance; Composite PES membranes; Electroactive membranes; Phase inversion

Received: December 4, 2015; *revised:* February 12, 2016; *accepted:* April 19, 2016

DOI: 10.1002/clen.201500953

1 Introduction

In recent years, nanoscale particles have been widely studied in prevention of environmental pollution and catalytic reactions because of their unrivaled physical, chemical, and antibacterial properties [1]. Their high surface area to volume ratio ensures more catalytic sites than bulk particles [2]. Due to the rapid development of science, nanocomposite materials which include organic–inorganic composites, nanopolymer matrix composites, and inorganic–inorganic composites have an important position for the development of new materials [3].

Nowadays, membrane processes are used intensively in order to supply of high-quality water for domestic and industrial demands, treatment and reuse of polluted water/wastewater, and removal of compounds from various industrial effluents [4–7]. Polyethersulphone (PES) membranes are the most common ones in wastewater treatment, due to its unique mechanical and structural durability, and chemical resistance. Besides these favorable properties, unfortunately PES is a hydrophobic material making its surface prone to fouling due to adsorptive mechanisms. Up to now, many studies have been made to improve the hydrophilic properties of the PES membrane surface. Therefore, various metal nanoparticles have been added to the polymer matrix due to reducing membrane fouling, and increasing membrane performance in terms of flux and selectivity [8]. Nanoparticle additive composite membranes are formed by the addition of inorganic oxide particles in a wide range from micrometer to nanometer sizes to the polymeric casting solution. Over the past few years, many types of nanoparticles such as Ag, TiO_2, Se, and Cu were used to prepare nanocomposite membranes [9–11].

The phase inversion process is a well-known technique to prepare asymmetric polymeric membranes [12–15]. Up to now, parameters such as polymer concentration in casting solutions [16], types of solvent/non-solvent pairs [17], cast film thickness [18], presence of additives [19], coagulation bath temperature [20], addition of nanoparticles [21], and the presence of solvents [22] have been tested to clarify the membrane formation mechanism and membrane morphology. For example, Maximous et al. reported polymer concentration as the most important parameter for membrane properties. It was found that with an increase in polymer concentration from 10 to 18%, the deionized water permeation decreased from 1227.4 to 866.5 L/(m^2 bar) per h. This result suggests that increased polymer concentration forms a thicker and denser skin layer. They extended this research using zirconia (ZrO_2) in order to increase chemical stability of membranes. Therefore, membranes

Correspondence: Dr. N. Dizge, Department of Environmental Engineering, Mersin University, 33343, Mersin, Turkey
E-mail: nadirdizge@gmail.com

Abbreviations: **AFM**, atomic force microscopy; **C-AFM**, conductive AFM; **CuNPs**, copper nanoparticles; **DLS**, dynamic light scattering; **EDX**, energy dispersive X-ray spectroscopy; **FE-SEM**, field emission SEM; **NMP**, N-methyl-2-pyrrolidone; **PES**, polyethersulfone; **rGO**, reduced grapheneoxide; **SEM**, scanning electron microscopy; **XRD**, X-ray diffraction.

© 2016 WILEY-VCH Verlag GmbH & Co. KGaA, Weinheim

are more suitable for liquid phase applications under severe conditions. The addition of ZrO_2 nanoparticles to the polymer casting solution improved the membrane strength, but slightly affected the membrane thickness. Although the zirconia blended membrane showed lower flux decline, fouling resistance (total and cake resistance) improved when compared to the unmodified membrane [23].

Safarpour et al. developed PES-based mixed matrix nanofiltration membranes by blending with partially reduced grapheneoxide (rGO)/TiO_2 nanocomposite [24]. The effect of rGO/TiO_2 content on the morphology and performance of the synthesized membranes was investigated by scanning electron microscopy (SEM), energy dispersive X-ray (EDX) spectroscopy, atomic force microscopy (AFM), and water contact angle analysis. It was reported that the blended membranes displayed improved water permeability and fouling resistance when compared to the neat PES. The water flux reached a maximum value (45.0 kg/m^2 h) when the content of rGO/TiO_2 was 0.15 wt%, while the neat PES membrane was 23.1 kg/m^2 h. Bovine serum albumin solution was used to test fouling resistance of the membranes and 0.1 wt% rGO/TiO_2 membrane showed the best antifouling property. Moreover, nanofiltration performance of the prepared membranes was tested for removal of three organic dyes with different molecular weights and the rGO/TiO_2/PES membranes showed better dye removal performance than the neat PES membranes [24].

Moghimifar et al. investigated antifouling properties of PES ultrafiltration membranes, prepared using NaX zeolite and TiO_2 nanoparticles as hydrophilic inorganic materials in order to separate oil-in-water emulsions [25]. Entrapping into the PES matrix and coating on the surface of the PES membranes using TiO_2 and zeolite nanoparticles were tested. The results showed that the entrapping method (TiO_2 and zeolite nanoparticles were blended into the polymer matrix with solution) provided decreasing of membrane fouling propensity. However, the ultrafiltration PES membranes indicated good separation performance and excellent antifouling properties by the coating technique [25].

Copper and copper alloys are the special materials which are also registered deliberately as Environmental Protection Agency (EPA) public health product. Moreover, copper is a cost-effective material and it is able to kill microbes quickly as well as it reduces microbial contamination effectively. For this reason, cheaper composite membrane production will be possible. Additionally, due to electroactive surface features of copper nanoparticles (CuNPs) blended membranes could supply inhibition of biofilm formation especially for electromembrane bioreactor applications, and increase membrane flux. The objective of this study, was to synthesize CuNPs with high specific surface area in the aqueous phase and to prepare composite PES membranes. CuNPs were added at different concentrations from 0.25 to 2.0% w/w to the casting solution to prepare electroactive and antibacterial CuNPs/PES composite membranes. The effect of CuNPs concentration on the PES membranes was investigated by field emission scanning electron microscopy (FE-SEM), atomic force microscopy (AFM), conductive AFM (C-AFM), contact angle goniometry, and four-point probe measurements.

2 Materials and methods

2.1 Synthesis of copper nanoparticles

Copper(II) chloride dihydrate ($CuCl_2 \cdot 2H_2O$) and hydrazine hydrate ($NH_2NH_2 \cdot H_2O$) were obtained from Merck. Metallic nanocopper clusters were synthesized by the sonochemical reduction of copper(II) hydrazine carboxylate Cu-$(N_2H_3COO)_2 \cdot 2H_2O$ complex in aqueous medium. The method was described in sufficient detail in a previous study [11].

2.2 Synthesis of neat PES and CuNPs/PES blended membranes

PES (PES ultrason E6020P with MW = 58 000 g/mol) was gently provided by BASF, Turkey. *N*-Methyl-2-pyrrolidone (NMP) was purchased from Sigma–Aldrich. Distilled water was obtained with the two-stage Millipore Direct-Q3UV purification system. Neat and CuNPs/PES blended membranes were synthesized according to the phase inversion method. Figure 1 shows the membrane formation process. PES beads (18%, w/w) were added slowly into the NMP solvent for neat PES membrane preparation and the solution was stirred at 60°C for 24 h to form a homogeneous solution. However, different ratios of CuNPs (0.25, 0.5, 1.0, 2.0%, w/w) were added in

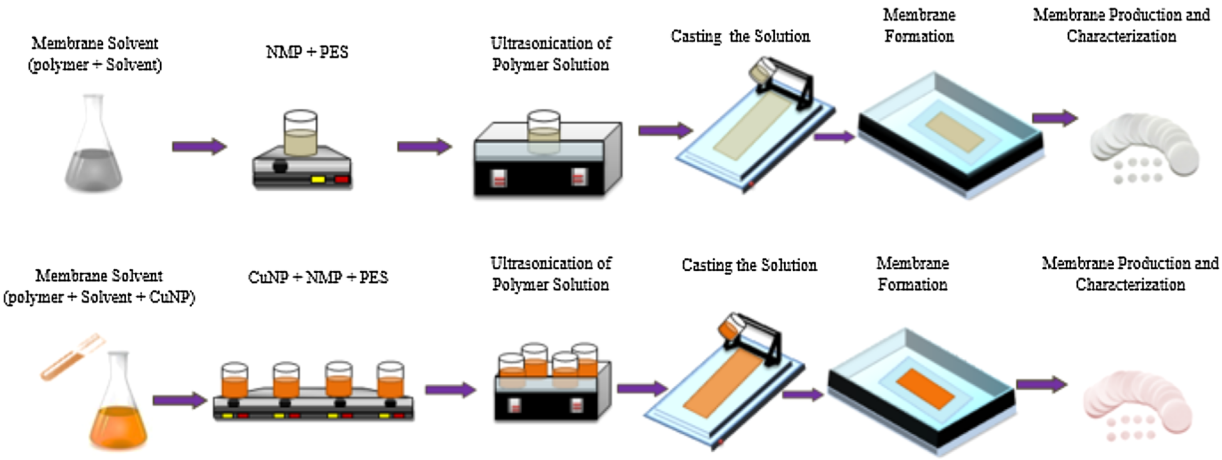

Fig. 1. Preparation of the neat and CuNPs/PES blended membranes using phase inversion method.

© 2016 WILEY-VCH Verlag GmbH & Co. KGaA, Weinheim

CLEAN Soil Air Water

NMP solvent using an ultrasonication bath for 15 min and PES beads (18%, w/w) were then poured to this solution for CuNPs/PES blended membrane preparation. The casting solutions were ultrasonicated for 10 min to remove air bubbles. Then, the casting solutions of neat PES and CuNPs/PES blended were spread with a casting knife gap setting of 200 μm at 100 mm/s casting shear on a glass plate. The casting films were kept 10 s for evaporation, and then the glass plates were immediately dipped in a deionized water bath to provide polymer precipitation. After membrane formation, the membranes were taken from the water bath and stored in fresh deionized water for at least 24 h to guarantee the complete phase inversion [11].

2.3 Microbial experimentation and antibacterial activity

Endo-agar used in preparing plates for antibacterial membrane test was purchased from Merck. All chemicals were used as received without further purification. Antibacterial efficacies of the CuNPs/PES membranes were examined with the Gram-negative *Escherichia coli* ATCC25922 bacteria culture. The pure bacteria culture was inoculated in a 500 mL flask with 100 mL of 0.9 g/L K_2HPO_4, 0.5 g/L KH_2PO_4, 0.5 g/L NH_4Cl, 0.1 g/L $CaCl_2 \cdot 2\ H_2O$, 0.2 g/L $MgCl_2 \cdot 6\ H_2O$, 0.1 g/L $FeCl_2 \cdot 4\ H_2O$ [26], 0.5 mg/L glucose, and 50 mg/L yeast. Bacteria were grown aerobically on minimal medium at 37°C overnight. The amount of *E. coli* bacteria was measured via standard plate count [27]. Endo-agar plates, which will not permit to grow bacteria species other than coliforms [28], were used to determine whether viable *E. coli* was on the CuNPs/PES blended membranes. Endo-agar plates were prepared according to Merck Microbiology Manual, 12th Edition. *E. coli* culture (100 mL) was filtered through CuNPs blended PES (0.25, 0.5, 1.0, 2.0%, w/w) and neat membranes. Circle pieces of neat and CuNPs blended PES membranes were gently placed over solidified agar Petri plates.

2.4 Characterization methods

Powder X-ray diffraction (XRD) measurements for CuNPs characterization were performed on a SmartLab Multipurpose Diffractometer with Cu K_α radiation ($\lambda = 1.5418$ Å). The samples were prepared by packing 5 mg of solid in a 10 mm length limited slit. Particle size distributions were obtained using a Malvern Zetasizer Nano ZS instrument.

FE-SEM images were recorded using a Zeiss/Supra 55 FE-SEM, and the samples were coated with platinum before the measurements.

AFM and C-AFM studies were carried out in non-contact mode using Park System XE-100 SPM, and topographic images were analyzed using Park Systems XEI software. An electrical conductive tip (Cr-Au) was used over the specified surface of the membrane in current detection AFM mode. In C-AFM mode, silver contact was used to pass current through the sample surface, a flowing current can be analyzed by an external electronic device. A conductive cantilever is brought in contact with the membrane surface. When it is attached to the silver layer upon application of a voltage between tip and sample; a flowing current can be analyzed by an external electronic device.

The contact angle is the angle, conventionally measured through the liquid, where a liquid/vapor interface meets a solid surface. KSV CAM 200 goniometer (KSV Instruments) was used for contact angle measurements of the neat and CuNPs/PES blended membranes. All contact angle measurements were made using 1 μL of deionized water. The analyses were performed at three different locations on the membrane surfaces.

The electric conductivity of the copper blended membranes was measured by Entek Four Point Prob device. The membrane was cut into 1 cm × 2 cm strips and all conductivity measurements were taken at room temperature (25 ± 1°C).

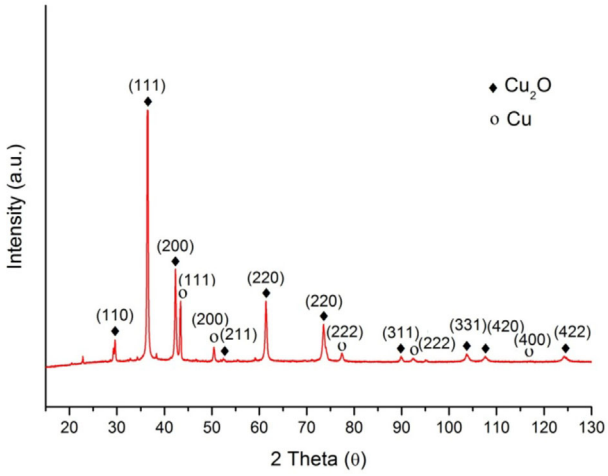

Fig. 2. XRD pattern of CuNPs.

3 Results and discussion

The main objectives of this study were to investigate electroactive and antibacterial properties of PES membranes containing CuNPs. This study was performed systematically as follows:

(1) Synthesis and characterization of CuNPs,

(2) Preparation and characterization of neat and CuNPs/PES blended membranes,

(3) Antibacterial performance evaluation of the electroactive membranes using *E. coli* as a model Gram-negative bacterium.

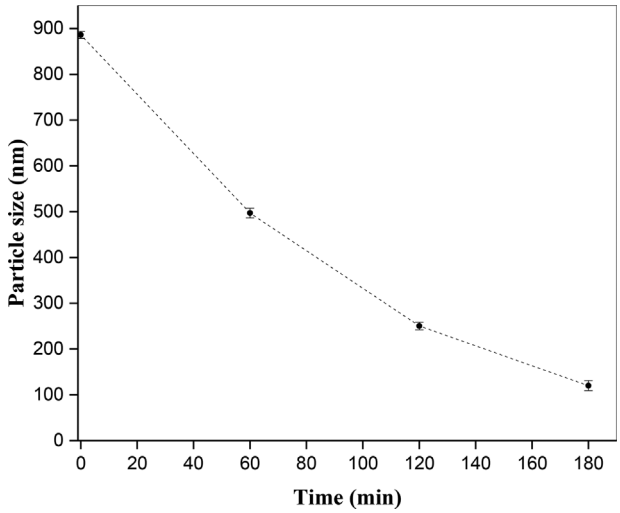

Fig. 3. Particle size distributions of CuNPs against time.

© 2016 WILEY-VCH Verlag GmbH & Co. KGaA, Weinheim

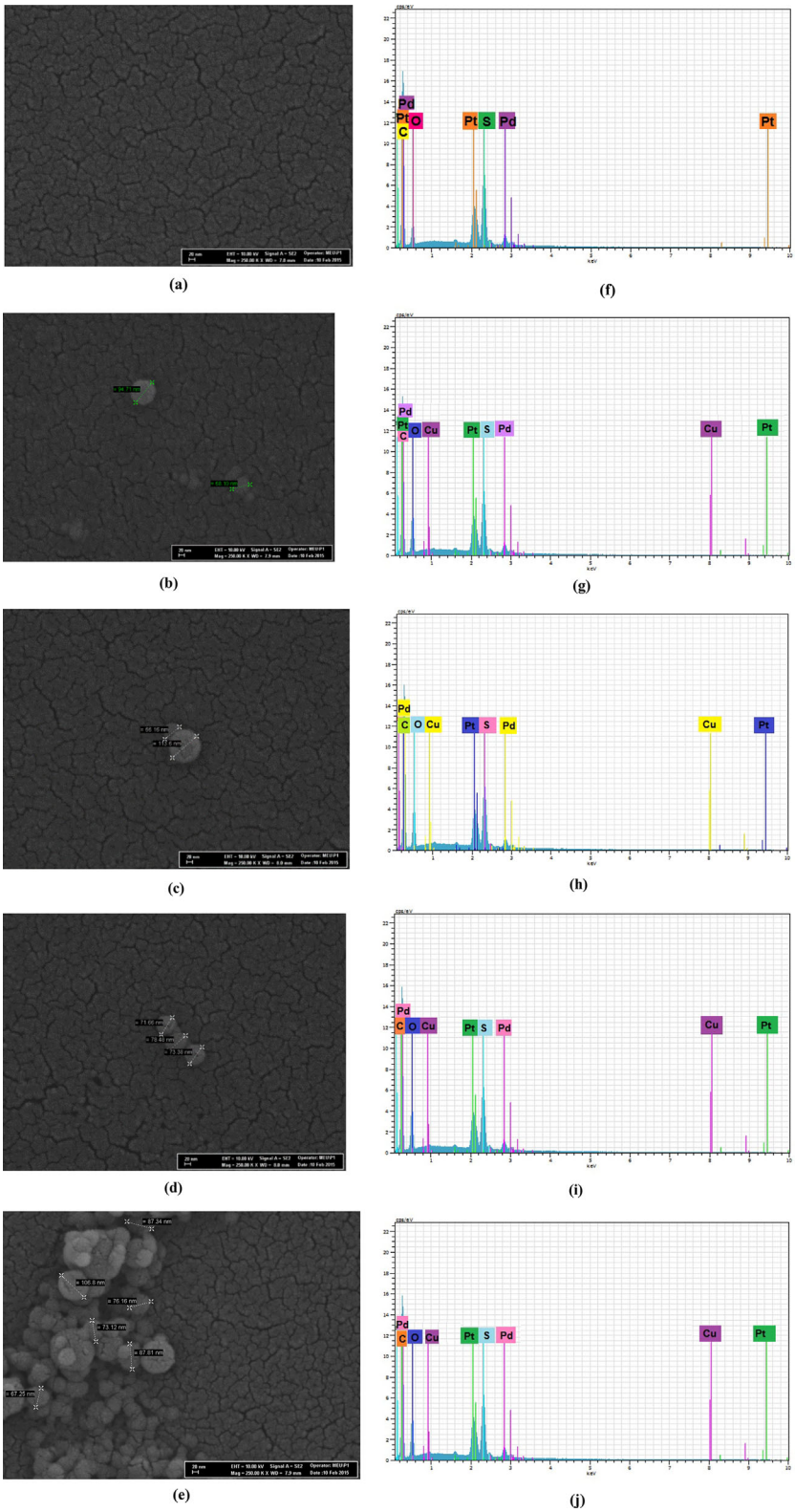

Fig. 4. (a–e) SEM images of the top layer surfaces, (f) EDX analysis of neat, and (g–j) CuNPs/PES blended membranes.

3.1 Characterization of copper nanoparticles

3.1.1 XRD

CuNPs were characterized using XRD. Figure 2 shows the XRD pattern of the nanopowder obtained after 180 min. The XRD pattern clearly shows the mixture formation of cuprous oxide (Cu_2O) and metallic copper (Cu) phases. The formation of zerovalent CuNPs can be explained by the chemical reduction of $CuCl_2 \cdot 2\ H_2O$ in the solution of hydrazine hydrate ($NH_2NH_2 \cdot H_2O$) [29]. It has been reported that in this reaction initially Cu^{2+} ions were reduced to Cu^{+} ions which precipitated as

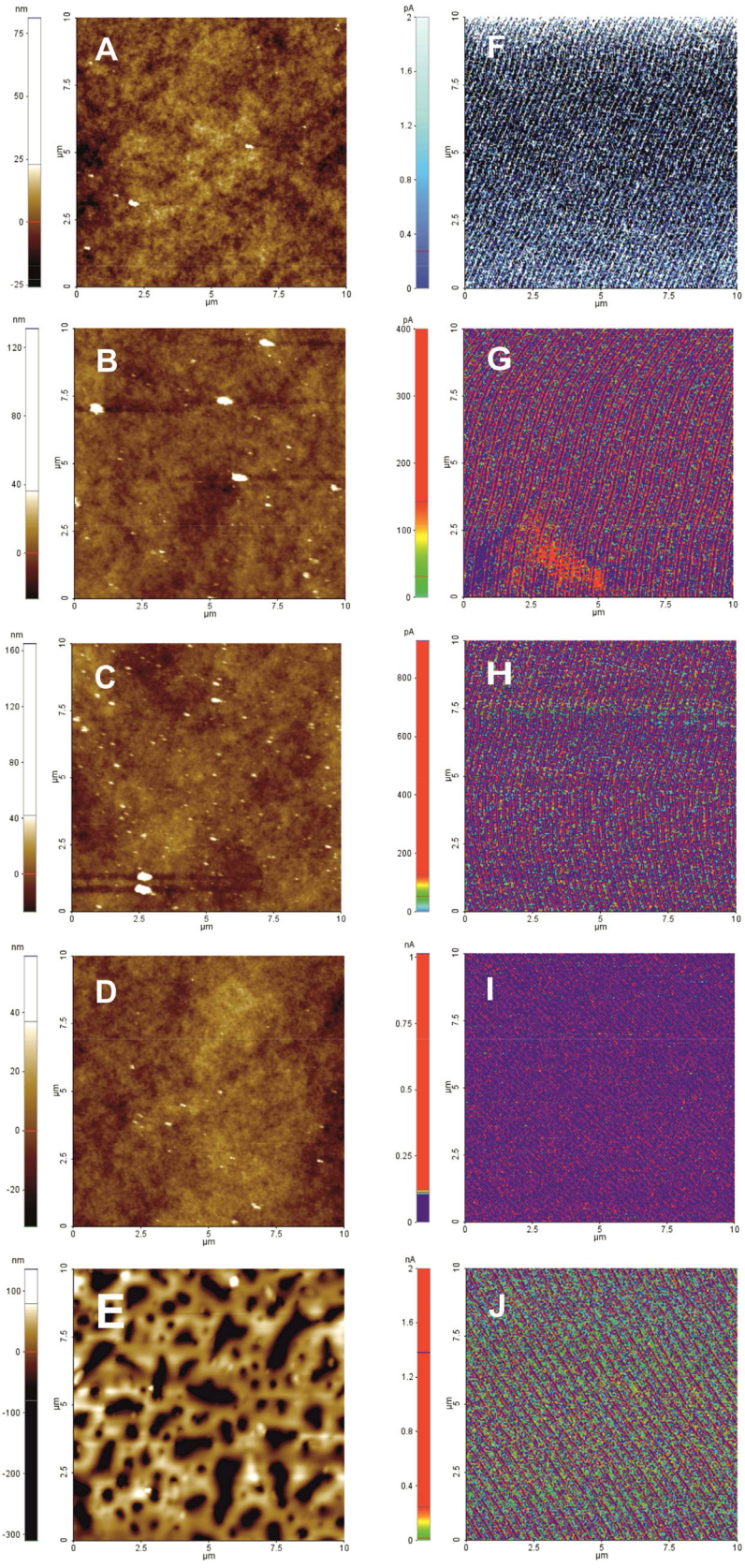

Fig. 5. AFM analysis of (A) neat membrane; (B–E) CuNPs blended membrane (0.25, 0.5, 1.0, 2.0% w/w); (F–J) corresponding current image measured by C-AFM.

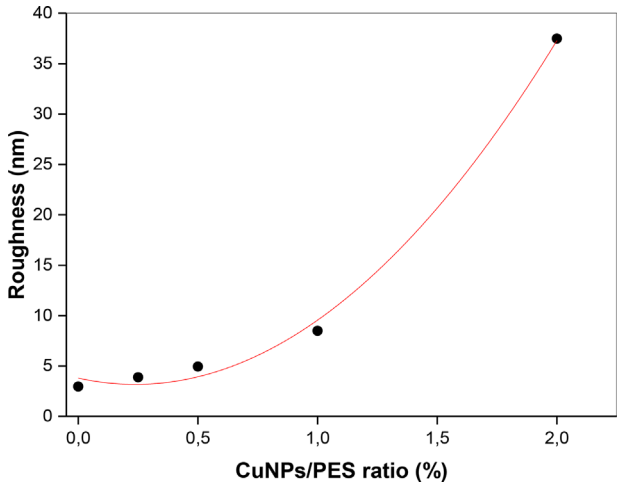

Fig. 6. The roughness graphs of neat and CuNPs/PES blended membranes.

Cu_2O particles, afterwards the reduction of cuprous oxide to copper metal powder occurred [30].

3.1.2 Particle size distribution

The size and uniformity of the nanoparticles were investigated by dynamic light scattering (DLS) technique using Malvern Zetasizer Nano ZS. For these measurements, the samples were diluted to 25 μg/mL CuNPs in distilled water and sonicated for 20 min prior to DLS analysis. Size distribution was obtained from the average of at least five runs. Figure 3 shows particle sizes of synthesized CuNPs samples against time. It was observed that the nanoparticle size decreased from 886 ± 7.7 to 120 ± 10.8 nm after 180 min. Agglomeration of nanoparticles during the reaction commonly occurring depends on surface charge and type of the nanoparticles. In this study, smaller particle sizes were obtained after 3 h ultrasonic irradiation.

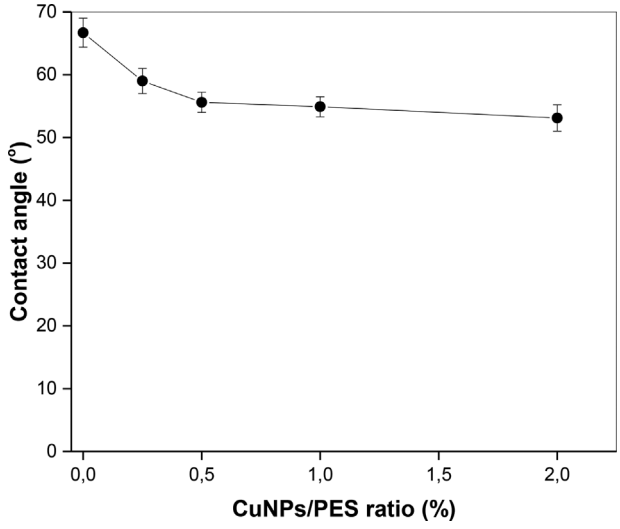

Fig. 7. The contact angle values of neat and CuNPs/PES blended membranes.

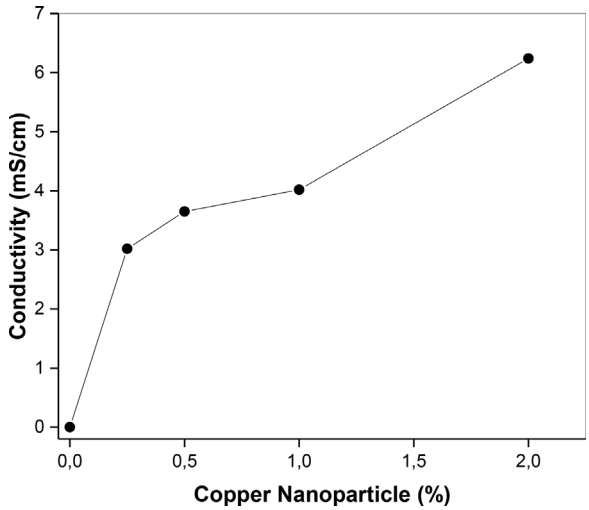

Fig. 8. The conductivity of the membranes containing different CuNPs concentrations.

3.2 Characterization of neat PES and CuNPs/PES blended membranes

The synthesized neat and CuNPs/PES blended membranes were characterized by using different techniques such as FE-SEM, AFM, C-AFM, contact angle goniometry, and four-point probe technique.

3.2.1 SEM Measurements

The surface morphologies of neat PES and CuNPs/PES blended membranes were investigated by FE-SEM in high vacuum mode after coating with platinum. FE-SEM images were taken to determine the effect of the CuNPs concentration on the membrane morphology. Figure 4a–e shows the FE-SEM images of the top layer surfaces of neat and CuNPs/PES blended membranes. Membrane pores can be observed as cracks for all membranes. SEM images of CuNPs blended membranes revealed the formation of round shape copper grown on the surface of these membranes. Each round shape nanoparticle has almost the same size in the range of 100 nm (approximately 65–115 nm). The membrane surface shown in Fig. 4b–e indicated that the nanoparticles were distributed on the membrane surface; however, some particles formed aggregates which increased when the nanoparticle concentration increased from 0.25 to 2.0%. Due to an intense concentration, nanoparticles aggregated during the phase inversion reaction and were deposited to the membrane surface. EDX spectra show high copper intensity, indicating that CuNPs entered into the membrane structure (Fig. 4g–j).

3.2.2 AFM and C-AFM Measurements

Surface morphology of CuNPs/PES blended membranes was also investigated by AFM. AFM analysis of neat and CuNPs blended PES membranes are shown in Fig. 5. These measurements clearly reveal that the formation of the membranes has a porous structure. However, it can be also seen that the 2% CuNPs blended membrane's surface has different pore shapes at different sizes. C-AFM studies were used for the investigation of electrical conductance ability of copper blended membranes [31–33]. C-AFM images display surface conductivity of copper blended membranes. As can be seen in Fig. 5,

© 2016 WILEY-VCH Verlag GmbH & Co. KGaA, Weinheim

membrane topography and its conductivity vary depending on the amount of CuNPs. Figure 5a–e shows AFM analysis of CuNPs (0, 0.25, 0.5, 1.0, 2.0%) blended membranes. The color scheme in Fig. 5f–j shifting from blue to red represents the conductivity order of the membrane surface. All blended membranes showed conductivity at nA level in nanoscale. Scanning on microscale regions with high current for determining the blended membranes can be differentiated from majority domains with lower current and non-conductive areas (Fig. 5f–j) [34]. Copper blended membranes showed different conductivities due to different amounts of CuNPs. As can be seen in Fig. 5f, the neat membrane did not show any conductivity.

Figure 6 shows the surface roughness graphs of CuNPs blended membranes obtained by AFM (scanned area: $10\,\mu m \times 10\,\mu m$). The roughness values of neat, 0.25% CuNPs/PES and 0.50% CuNPs/PES blended membranes were same, but 1.0% CuNPs/PES and 2.0% CuNPs/PES nanocomposite membranes had highest roughness values (Fig. 6). The roughness value of the neat, 0.25, and 0.50% CuNPs/PES blended membranes were 2.95, 3.88, 4.93 nm, respectively. However, 1.0 and 2.0% CuNPs/PES blended membranes were 8.49 and 37.48 nm, respectively. The addition of CuNPs increased the roughness value when compared with neat PES membrane. The reason of this can be explained by increased CuNPs aggregation onto PES blended membrane surface with increasing CuNPs ratio, and therefore, causing rougher surface.

3.2.3 Contact angle measurements

The contact angle values of neat and CuNPs/PES blended membranes at different concentrations (0.25, 0.5, 1.0, 2.0%, w/w) are given in Fig. 7. The contact angle of neat PES membrane decreased with the addition of CuNPs from 66.7 ± 2.3 to $53.1 \pm 2.1°$. It was found that the contact angle of all CuNPs blended membranes ensured hydrophilicity when compared to the neat PES membranes. The hydrophilicity of the CuNPs blended membrane may increase with increasing membrane porosity, which caused the migration of CuNPs to the membrane surface during the phase inversion process.

3.2.4 Conductivity measurements

Conductivity of the copper blended membranes was measured by using a four-point probe technique. To determine conductivity of copper blended membranes and optimize the doping process, monitoring of membrane conductivity exposure to CuNPs was performed. Membrane conductivity results are shown in Fig. 8. The conductivity of the membranes measured at room temperature changed in the range from 3 to 7 mS/cm. The conductivity increased with the increasing amount of copper ratio in the membrane up to the maximum value of 6.3 mS/cm.

3.3 Antibacterial study of neat and CuNPs/PES blended membranes with *E. coli*

Each antibacterial experiment was conducted in duplicate. The results showed that no bacteria were detected at the collected effluent from membrane filtrates, while the bacterial load of the influent was about 1.2×10^6 colony forming units (CFU)/mL. Observed bacterial growth on neat membranes, placed on endo-agar plates, growth was numerous (Fig. 9a). A notable decline in the number of bacteria was observed at 0.25 and 0.50% w/w CuNPs/PES blended membrane plates (Fig. 9b). On the contrary, the number of bacteria was almost zero on CuNPs/PES blended membranes with 1.0 and 2.0% w/w CuNPs (Fig. 9c). Inactivation of bacteria by CuNPs/PES blended membranes may involve killing or inactivating the bacteria by CuNPs. Even 0.25% CuNPs blended PES membranes have enough effect to reduce the number of bacteria. Antibacterial activity of CuNPs/PES blended membranes increased when CuNPs concentration increased from 0.25 to 2.0%. Excess copper can cause a decline in the membrane integrity of *E. coli*. Grass et al. reported that bacteria, yeasts, and viruses are rapidly killed on metallic copper surfaces. The *E. coli* cell membrane tears off due to CuNPs situated on the membrane surface as well as other stress phenomena, leading to loss of cell membrane potential, and cytoplasmic content [35]. Therefore, it is concluded that CuNPs/PES blended membranes effectively inhibit bacteria growth.

The study performed by Wilks et al. showed that oxidative stress was an important factor that influenced bacterial cell survival on metallic copper [36]. Constitution of reactive oxygen species contributing to contact killing is mediated by redox cycling between the different copper species such as Cu(0), Cu(I), and Cu(II) [35–37].

4 Concluding remarks

In this study, neat PES and CuNPs/PES blended membranes were prepared, and tested at antibacterial performance. The XRD pattern clearly showed the a mixture of cuprous oxide (Cu_2O) and metallic copper (Cu) phases are formed with this method. Moreover, the particle size of synthesized CuNPs samples was approximately 120 ± 10.8 nm. C-AFM images displayed surface conductivity of

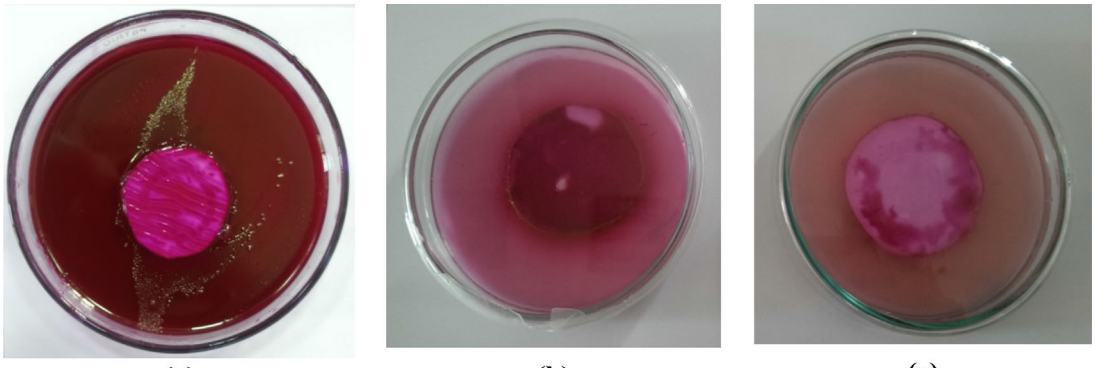

Fig. 9. Study of *E. coli* activity of (a) neat membrane, (b) 0.25% CuNPs blended membrane, (c) 1.0% CuNPs blended membrane.

© 2016 WILEY-VCH Verlag GmbH & Co. KGaA, Weinheim

copper blended membranes and all blended membranes showed conductivity at nA level. The conductivities of the CuNPs blended membranes were measured in the range from 3 to 7 mS/cm. At the bacterial analysis, the growth of bacterial colonies decreased with increasing CuNPs ratio and CuNPs/PES blended membranes effectively inhibited bacterial growth. Additionally, we are currently working on electro membrane bioreactor systems to decrease biofilm formation and to increase membrane flux by CuNPs blended membranes.

The authors have declared no conflict of interest.

References

[1] A. T. Bell, The Impact of Nanoscience on Heterogeneous Catalysis, *Science* **2003**, *299 (5613)*, 1688–1691.

[2] P. H. Reza, K. M. Hossein, Y. M. Hasan, S. Arash, Z. Abbas, Photodegradation Of HMX And RDX In The Presence Of Nanocatalyst Of Zinc Sulfide Doped With Copper, *Iran. J. Chem. Chem. Eng*. **2009**, *28 (4)*, 13–19.

[3] L. S. Wang, R. Y. Hong, Synthesis, surface modification, and characterization of nanoparticles, *Advances in nanocomposites—Synthesis, Characterization, and Industrial applications*. (Ed.: B. Reddy), InTech, Rijeka, Croatia **2011**, pp. 289–322.

[4] M. I. Shahidul, C. M. Wanik, Nanopore Membrane in Water Treatment Chemical Reclamation: A Pilot Study towards Environmental Sustainability, *Manuf. Oper. Res. Sustainability* **2013**, *1 (1)*, 7–12.

[5] T. Coskun, A. Yildirim, C. Balcik, N. M. Demir, E. Debik, Performances of Reverse Osmosis Membranes for Treatment of Olive Mill Wastewater, *Clean—Soil Air Water* **2013**, *41 (5)*, 463–468.

[6] H. E. Van, J. Verbauwhede, F. Vanlerberghe, S. Demunter, J. Cabooter, Treating Different Types of Raw Water with Micro and Ultrafiltration for Further Desalination Using Reverse Osmosis, *Desalination* **1998**, *117*, 49–60.

[7] Y. Z. Xu, E. L. Remi, Treatment of Textile Dye Plant Effluent by Nanofiltration Membrane, *Sep. Sci. Technol*. **1999**, *34 (13)*, 2501–2519.

[8] H. L. Richards, P. G. L. Baker, E. Iwuoha, Metal Nanoparticle Modified Polysulfone Membranes for Use in Wastewater Treatment: A Critical Review, *J. Surf. Eng. Mater. Adv. Technol*. **2012**, *2*, 183–193.

[9] M. S. Yuksel, B. Tas, D. Y. Koseoglu-Imer, I. Koyuncu, Effect of Silver Nanoparticle (agnp) Location in Nanocomposite Membrane Matrix Fabricated with Different Polymer Type on Antibacterial Mechanism, *Desalination* **2014**, *347*, 120–130.

[10] M. S. Jyothi, M. Padaki, R. G. Balakrishna, R. K. Pai, Synthesis and Design of Psf/tio2 Composite Membranes for Reduction of Chromium (vi): Stability and Reuse of the Product and the Process, *J. Mater. Res*. **2014**, *29 (14)*, 1537–1545.

[11] N. Akar, B. Asar, N. Dizge, I. Koyuncu, Investigation of Characterization and Biofouling Properties of Pes Membrane Containing Selenium, and Copper Nanoparticles, *J. Membr. Sci*. **2013**, *437*, 216–226.

[12] M. J. Han, S. T. Nam, Thermodynamic and Rheological Variation in Polysulfone Solution by Pvp, and Its Effect in the Preparation of Phase Inversion Membrane, *J. Membr. Sci*. **2002**, *202*, 55–61.

[13] W. Y. Chuang, T. H. Young, W. Y. Chiu, C. Y. Lin, The Effect of Polymeric Additives on the Structure and Permeability of Poly (vinyl Alcohol) Asymmetric Membranes, *Polymer* **2000**, *41*, 5633–5641.

[14] J. H. Kim, K. H. Lee, Effect of Peg Additive on Membrane Formation by Phase Inversion, *J. Membr. Sci*. **1998**, *138*, 153–163.

[15] E. Saljoughi, T. Mohammadi, Cellulose Acetate (ca)/polyvinylpyrrolidone (pvp) Blend Asymmetric Membranes: Preparation, Morphology, and Performance, *Desalination* **2009**, *249*, 850–854.

[16] H. J. Kim, R. K. Tyagi, A. E. Fouda, K. Ionasson, The Kinetic Study for Asymmetric Membrane Formation via Phase-inversion Process, *J. Appl. Polym. Sci*. **1996**, *62*, 621–629.

[17] S. S. Madaeni, A. Rahimpour, Effect of Type of Solvent and Nonsolvents on Morphology and Performance of Polysulfone, and Polyethersulfone Ultrafiltration Membranes for Milk Concentration, *Polym. Adv. Technol*. **2005**, *16*, 717–724.

[18] N. Vogrin, C. Stropnik, V. Musil, M. Brumen, The Wet Phase Separation: The Effect of Cast Solution Thickness on the Appearance of Macrovoids in the Membrane Forming Ternary Cellulose Acetate/Acetone/Water System, *J. Membr. Sci*. **2002**, *207*, 139–141.

[19] I. C. Kim, K. H. Lee, Effect of Various Additives on Pore Size of Polysulfone Membrane by Phase-Inversion Process, *J. Appl. Polym. Sci*. **2003**, *89*, 2562–2566.

[20] H. A. Tsai, R. C. Ruaan, D. M. Wang, J. Y. Lai, Effect of Temperature and Span Series Surfactant on the Structure of Polysulfone Membranes, *J. Appl. Polym. Sci*. **2002**, *86*, 166–173.

[21] S. Kim, M. Marion, B. H. Jeong, E. M. V. Hoek, Crossflow Membrane Filtration of Interacting Nanoparticle Suspensions, *J. Membr. Sci*. **2006**, *284 (1–2)*, 361–372.

[22] J. Y. Lai, F. C. Lin, C. C. Wang, D. M. Wang, Effect of Nonsolvent Additives on the Porosity and Morphology of Asymmetric Tpx Membranes, *J. Membr. Sci*. **1996**, *118*, 49–61.

[23] N. Maximous, G. Nakhla, W. Wan, K. Wong, P Erformance of a Novel ZrO2/PES Membrane for Wastewater Filtration, *J. Membr. Sci*. **2010**, *352 (1–2)*, 222–230.

[24] M. Safarpour, V. Vatanpour, A. Khataee, Preparation and Characterization of Graphene Oxide/TiO2 Blended PES Nanofiltration Membrane With Improved Antifouling, and Separation Performance, *Desalination* **2015**, DOI: 10.1016/j.desal.2015.07.003

[25] V. Moghimifar, A. Esmaili Livari, A. Raisi, A. Aroujalian, Enhancing the Antifouling Property of Polyethersulfone Ultrafiltration Membranes Using NaX Zeolite and Titanium Oxide Nanoparticles, *RSC Adv*. **2015**, *5*, 55964–55976.

[26] A. E. Tugtas, S. G. Pavlostathis, Electron Donor Effect on Nitrate Reduction Pathway and Kinetics in a Mixed Methanogenic Culture, *Biotechnol. Bioeng*. **2007**, *98 (4)*, 756–763.

[27] C. H. Collins, P. M. Lyne, J. M. Grange, *Collins and Lyne's Microbiological Methods*, 7th ed, Butterworth Heinemann, Oxford, UK **1995**. p. 149.

[28] K. W. v. Drigalski, H. Conradi, Über Ein Verfahren Zum Nachweis Der Typhusbacillen, *Z. Hyg. Infektionskrankh*. **1902**, *39 (1)*, 283–300.

[29] M. Aslam, G. Gopakumar, T. L. Shoba, I. S. Mulla, K. Vijayamohanan, S. K. Kulkarni, J. Urban, et al. Formation of Cu and Cu2o Nanoparticles by Variation of the Surface Ligand: Preparation, Structure, and Insulating-To-Metallic Transition, *J. Colloid Interface Sci*. **2002**, *255*, 79–90.

[30] P. Chokratanasombat, E. Nisaratanaporn, Preparation of Ultrafine Copper Powders with Controllable Size via Polyol Process with Sodium Hydroxide Addition, *Eng. J*. **2012**, *16*, 39–46.

[31] D. Moerman, N. Sebaihi, S. E. Kaviyil, P. Leclere, R. Lazzaroni, O. Douheret, Towards a Unified Description of the Charge Transport Mechanisms in Conductive Atomic Force Microscopy Studies of Semiconducting Polymers, *Nanoscale* **2014**, *6*, 10596–10603.

[32] C. Hentschel, L. Jiang, D. Ebeling, J. C. Zhang, X. Chenand, L. F. Chi, Conductance Measurements of Individual Polypyrrole Nanobelts, *Nanoscale* **2015**, *7*, 2301–2305.

[33] S. Sengupta, D. Ebeling, S. Patwardhan, X. Zhang, H. von Berlepsch, C. Böttcher, V. Stepanenko, et al. B Iosupramolecular Nanowires from Chlorophyll Dyes with Exceptional Charge-transport Properties, *Angew. Chem. Int*. **2012**, *51 (26)*, 6378–6382.

[34] R. Hiesgen, E. Aleksandrov, G. Meichsner, I. Wehl, E. Roduner, K. A. Friedrich, High-resolution Imaging of Ion Conductivity of Nafion® Membranes with Electrochemical Atomic Force Microscopy, *Electrochim Acta* **2009**, *55*, 423–429.

[35] G. Grass, C. Rensing, M. Solioz, M Etallic Copper as an Antimicrobial Surface, *Appl. Environ. Microbiol*. **2011**, *77 (5)*, 1541–1547.

[36] S. A. Wilks, H. Michels, C. W. Keevil, The Survival of *Escherichia Coli* O157 on a Range of Metal Surfaces, *Int. J. Food Microbiol*. **2005**, *105 (3)*, 445–454.

[37] C. Espirito Santo, N. Taudte, D. H. Nies, G. Grass, Contribution of Copper Ion Resistance to Survival of *Escherichia Coli* on Metallic Copper Surfaces, *Appl. Environ. Microbiol*. **2008**, *74*, 977–986.